Muscle-regulated expression and determinants for neuromuscular junctional localization of the mouse RIα regulatory subunit of cAMP-dependent protein kinase

Sébastien Barradeau, Tereza Imaizumi-Scherrer, Mary C. Weiss*, and Daniela M. Faust

Unité de Génétique de la Différenciation, Département de Biologie Moléculaire, Institut Pasteur, Unité de Recherche Associée 1773 du Centre National de la Recherche Scientifique, 25, Rue du Dr Roux, 75724 Paris Cedex 15, France

Edited by Susan S. Taylor, University of California at San Diego, La Jolla, CA, and approved February 20, 2001 (received for review August 17, 2000)

In skeletal muscle, transcription of the gene encoding the mouse type Iα (RIα) subunit of the cAMP-dependent protein kinase is initiated from the alternative noncoding first exons 1a and 1b. Here, we report that activity of the promoter upstream of exon 1a (Pa) depends on two adjacent E boxes (E1 and E2) in NIH 3T3-transfected fibroblasts as well as in intact muscle. Both basal activity and MyoD transactivation of the Pa promoter require binding of the upstream stimulating factors (USF) to E1. E2 binds either an unknown protein in a USF/E1 complex-dependent manner or MyoD. Both E2-bound proteins seem to function as repressors, but with different strengths, of the USF transactivation potential. Previous work has shown localization of the RIα protein at the neuromuscular junction. Using DNA injection into muscle of plasmids encoding segments of RIα or RIIα fused to green fluorescent protein, we demonstrate that anchoring at the neuromuscular junction is specific to RIα subunits and requires the amino-terminal residues 1–81. Mutagenesis of Phe-54 to Ala in the full-length RIα–green fluorescent protein template abolishes localization, indicating that dimerization of RIα is essential for anchoring. Moreover, two other hydrophobic residues, Val-22 and Ile-27, are crucial for localization of RIα at the neuromuscular junction. These amino acids are involved in the interaction of the *Caenorhabditis elegans* type Iα homologue R_{CE} with $AKAP_{CE}$ and for *in vitro* binding of RIα to dual A-kinase anchoring protein 1. We also show enrichment of dual A-kinase anchoring protein 1 at the neuromuscular junction, suggesting that it could be responsible for RIα tethering at this site.

Subcellular localization is a crucial mechanism to achieve optimal activation and substrate specificity of the cAMP-dependent protein kinase (PKA, EC 2.7.1.37). PKA type II targeting to subcellular structures and organelles or assembly in signaling complexes is a result of tethering of RII regulatory (R) subunits by members of the A-kinase anchoring protein (AKAP) family, a group of structurally divergent proteins possessing a conserved RII-binding site (1, 2).

Although a large proportion of type Iα R subunit (RIα) is dispersed in the cytosol, it also is associated with the plasma membrane of human erythrocytes (3), recruited to the "cap site" of activated T lymphocytes (4) and sequestered along the fibrous sheath of mammalian spermatozoa (5). In addition, we have demonstrated previously the accumulation of RIα at the neuromuscular junction (NMJ) of skeletal muscle (6) and its association with microtubules (7). The high affinity RII-binding sites of certain AKAPs, named dual (D)-AKAPs, also sequester RIα *in vitro* but with a 25–500 lower affinity (8, 9). Thus, type I PKA also could be anchored in intact cells through specific AKAP-RIα interactions. In fact, Angelo and Rubin (10) have identified $AKAP_{CE}$ from *Caenorhabditis elegans*, which binds the R_{CE} subunit. Because R_{CE} is closely related to mammalian RIα, $AKAP_{CE}$ is the first eukaryotic RI-specific tethering protein. Indeed, $AKAP_{CE}$ binds mammalian RIα but not RII subunits (10, 11).

To define the structural determinants necessary for NMJ localization of the mouse RIα protein, we used *in vivo* plasmid injection into adult muscle as described by Wolff *et al.* (12). The first 81 residues of RIα are sufficient to accumulate a green fluorescent (GFP) fusion protein at the NMJ, indicating that anchoring requires the dimerization/docking domain. NMJ localization is specific for RIα because the corresponding docking region of RIIα (residues 1–44) does not confer accumulation. The localization of RIα is affected by mutation of the conserved residues Val-22, Ile-27, and Phe-54, which are essential for the interaction of R_{CE} with $AKAP_{CE}$ (11) and for RIα binding to D-AKAP1 *in vitro* (13). In fact, we observed an enrichment of D-AKAP1 at the NMJ, implying that RIα could be recruited by this anchoring protein.

RIα transcripts as well as the corresponding protein are enriched at the NMJ (6). Furthermore, we have described five alternative, noncoding first exons (1a–1e) for mouse RIα transcripts, and only those containing exons 1a and 1b are expressed in skeletal muscle (14). We investigated whether muscle-specific regulatory elements are implicated in transcriptional activity of the cognate exon 1a (Pa) and 1b (Pb) promoters. Muscle-specific gene regulation depends on E boxes (CANNTG) (15, 16). Basic helix–loop–helix (bHLH) or bHLH-leucine zipper proteins, such as the myogenic factors (MyoD, myf5, myogenin, and MRF4) (17) and the upstream stimulating factors (USF1, 2a and 2b) (18), bind to E box motifs according to the nature of the two variable NN nucleotides. Here, we show that two E boxes, which bind either USF or MyoD, control muscle-enhanced activity of the Pa promoter of the otherwise ubiquitously expressed RIα gene.

Materials and Methods

Reporter Gene Constructs and Site-Directed Mutagenesis. A 1.1-kb fragment (Pa) comprising the presumed mouse RIα exon 1a promoter and exon 1a ($-4{,}258$ to $-3{,}161$ nt) was amplified with primer pairs containing Sal*I* or Nco*I* restriction sites and cloned into plasmid pSKT-nLacZ, provided by S. Tajbakhsh (Institut Pasteur), resulting in plasmid Pa-nLacZ. To generate Pb-nLacZ, the 0.45-kb fragment including exon 1b and its upstream se-

This paper was submitted directly (Track II) to the PNAS office.

Abbreviations: PKA, cAMP-dependent protein kinase; R, regulatory; AKAP, A-kinase anchoring protein; NMJ, neuromuscular junction; D-AKAP, dual-AKAP; AChR, acetylcholine receptor; bHLH, basic helix–loop–helix; USF, upstream stimulating factor; EMSA, electrophoretic mobility-shift assay; GFP, green fluorescent protein; β-gal, β-galactosidase; mckR, muscle creatine kinase right E box; MLP, major late promoter.

*To whom reprint requests should be addressed. E-mail: mweiss@pasteur.fr.

The publication costs of this article were defrayed in part by page charge payment. This article must therefore be hereby marked "*advertisement*" in accordance with 18 U.S.C. §1734 solely to indicate this fact.

CELL BIOLOGY

quence (−3,162 to −2,710 nt) was amplified. The plasmid mδ(−839/+45)nLacZ, containing the β-galactosidase (β-gal) gene under control of the mouse acetylcholine receptor (AChR) δ-subunit promoter (19), was provided by L. Schaëffer (Ecole Normale Supérieur, Lyon, France).

To obtain GFP fusion proteins, the coding region of mouse RIα (14) was amplified from a full-length cDNA clone with the forward primer RIα/HIII (5′-TCTCGAGCTCAAGCTTAC-CACACCGAGAACCATGGCG-3′) and the reverse primers RIα/BI (5′-GGTGGCGATGGATCCGCAGGACAGGGA-CACGAAGC-3′) or RIα(1–91)/BI (5′-GGTTGGCGATG-GATCCGCCCTTCACCACTGGATTGGG-3′) or RIα(1–81)/BI (5′-GGTGGCGATGGTCCCTCGTCCTCCCTC-AGTCAGT-3′). The primers RIIα/HIII (5′-TCTGAGCT-CAAGCTTATGAGCCACATCCAGATCCCGCCGGGG-3′) and RIIα/BI (5′-GTGCGGACGCGCTCCGGGCGGCGG-GATCCTAGCGGTGGTAC-3′) were used to amplify the sequence encoding the first 44 residues from a human RIIα cDNA, given by K. Taskén (University of Oslo, Oslo, Norway). The PCR products were digested with Bam*HI* and Hin*dIII* and ligated into the vector pEGFP-N3 (CLONTECH). The resulting expression vectors, pRIα-, pRIα(1–91)-, pRIα(1–81)-, and pRIIα(1–44)-GFP, contain an in-frame fusion of RIα or RIIα to the 5′ end of the GFP cDNA under control of the human cytomegalovirus promoter.

Plasmids pE1m, pE2m, pE3m (single E box-mutated), pE21m, pE31m, pE32m (two mutated E boxes), and pE321m (mutations in the three E boxes) were obtained from Pa-nLacZ by mutagenesis using the QuickChange Site-Directed Mutagenesis kit (Stratagene) and mutation primers (Fig. 1*B*). The double-stranded primers C18A (5′-CGGAGTCTCCGGGAAGC-CGAGCTCTATGTGCAG-3′), V22A (5′-GAATGC-GAGCTCTATGCGCAGAAGCACAATATC-3′), I27A (5′-GTGCAGAAGCACAATGCCCAGGCCCTGCTGAAG-3′), and F54A (5′-CCTTCGGGAATACGCTGAGAGGTTG-GAGAAG-3′) were used to mutate Cys-18, Val-22, Ile-27, and Phe-54 to Ala, generating the pRIα(C18A)-, pRIα(V22A)-, pRIα(I27A)-, and pRIα(F54A)-GFP plasmids, respectively. Amino acids are numbered as in the European Molecular Biology Laboratory sequence database (14). All plasmids were verified by sequencing.

Cell Lines, Culture Conditions, and Transient Expression Assays. Mouse NIH 3T3 fibroblasts were grown in DMEM supplemented with 10% FCS. Mouse C2/7 myoblasts derived from the C2 skeletal muscle line were grown to confluence in DMEM with 20% FCS and induced to differentiate into myotubes by serum starvation (20).

Cells were transfected by the calcium phosphate procedure (21) with 5 μg of β-gal reporter constructs and 1 μg of a reporter containing the simian virus 40 early promoter linked to the luciferase gene (pGL2; Promega) in combination with different amounts of the MyoD expression plasmid, pEMSV-MyoD, provided by M. Lemonnier (Institut Pasteur), or vector lacking the MyoD coding sequence. The ΔbT1 expression vector encoding a dominant-negative form of USF1, deficient in DNA binding, and the TDU1 construct expressing transactivation domain-truncated USF1 proteins (22) were given by B. Viollet (Institut Cochin de Génétique Moléculaire, Paris). β-Gal activity was measured by a chemiluminescent reporter gene assay (Galacto-Light; Perkin–Elmer) and corrected by the luciferase activity (21).

Nuclear Extracts and Electrophoretic Mobility-Shift Assays (EMSA). EMSA reactions (20) were performed with nuclear extracts (23) from NIH 3T3 or myotube stage C2/7 cells and double-stranded oligonucleotides encompassing either wild-type or mutated E boxes of the Pa (Fig. 1*B*), the muscle creatine kinase (mckR) (17), or the adenovirus major late promoter (MLP) (24). Monoclonal anti-MyoD (Dako) and polyclonal anti-USF antibodies, given by B. Viollet, were used for supershift assays.

***In Vivo* DNA Injection into Skeletal Muscle.** β-Gal test or GFP fusion plasmids were resuspended in Mg^{2+}- and Ca^{2+}-free PBS (3 μg/μl). The *tibialis anterior* muscles of 3-week-old C57/BL6j × SJL mice were injected (12) with 45 μg of both β-gal test and pGL2 control plasmids for transient *in vivo* expression. Five days later, total muscle proteins were extracted and used to determine β-gal activities (25), which were corrected for the luciferase activity. Muscles, injected with the GFP fusion constructs (90 μg), were fixed in 4% formaldehyde, rinsed, and incubated with tetramethylrhodamine B isothiocyanate-α-bungarotoxin (1:500) for 30 min to label the NMJ. Fibers were mounted with Immuno-mount (Shandon, Pittsburgh) and examined with a photomicroscope (Zeiss).

Immunohistochemistry. Immunohistochemistry was performed on adult *tibialis anterior* muscle sections with an anti-D-AKAP1 polyclonal antibody (1:100) directed against the core domain of the protein (26), a gift of S. S. Taylor (University of California at San Diego, La Jolla). Images were acquired by confocal microscopy and analyzed as described (6).

Results and Discussion

E and N Box Motifs Are Present Upstream of RIα Exon 1a. Mouse RIα transcripts contain five alternative first exons (14). Fragments Pa to Pe (Fig. 1*A*) exhibit promoter activity when tested in transfected hepatoma and fibroblast cells (data not shown). Because muscle expresses exon 1a and 1b transcripts (14), a computer-assisted search for elements that could account for muscle-specific regulation was carried out on the Pa and Pb sequences. Both sequences contain multiple consensus binding sites for ubiquitous transcription factors (Sp1, AP-1, AP-2, and NF-1). In addition, Pa contains three E boxes located at 61 (E1), 81 (E2), and 203 nt (E3) upstream of the most 5′ transcription start site (Fig. 1*B*). Expression of skeletal muscle-specific genes, such as the α-subunit of AChR (27), is controlled primarily by MyoD, myogenin, and other E box-binding bHLH factors specific for the muscle lineage (15, 16). Pa also contains one N box (CCGGAA) at −286 nt; such a motif is required for the differential transcriptional regulation of AChR subunit genes in synaptic vs. extrasynaptic regions of muscle fibers (28).

The RIα Pa Promoter Is Highly Active in Intact Muscles. The ability of the Pa promoter to control expression in muscle was investigated by *in vivo* Pa-nLacZ plasmid injection into *tibialis anterior* muscles of 3-week-old mice. The β-gal reporter gene driven by Pa (Fig. 1*C*) exhibited a high activity in total extracts of nonregenerating muscle. In contrast, the δ-AChR promoter construct showed no detectable activity, as described for the α-AChR promoter (29).

In situ hybridizations on muscle sections of newborn mice by using specific probes for exon 1a or 1b showed weak signals throughout the muscle tissue. In addition, the exon 1a probe was enriched strongly at the NMJ (data not shown), as AChR subunit transcripts (30, 31). *In situ* cytochemical staining for β-gal activity in plasmid-injected muscle fibers, used to test the ability of N box elements to direct transcription in subjunctional nuclei (19, 32, 33), revealed no preferential sites of expression of the reporter gene driven by either the RIα Pa or Pb promoters alone or in different combinations with the other RIα promoters (data not shown). Staining appeared rapidly (45 min to 2 h) and concerned a large number of nuclei, and the number of positive fibers was high (up to 800 per muscle) for both the Pa- and Pb-nLacZ plasmids; in contrast, injection of muscles with the δ-AChR promoter plasmid resulted in only 20–50 positive fibers

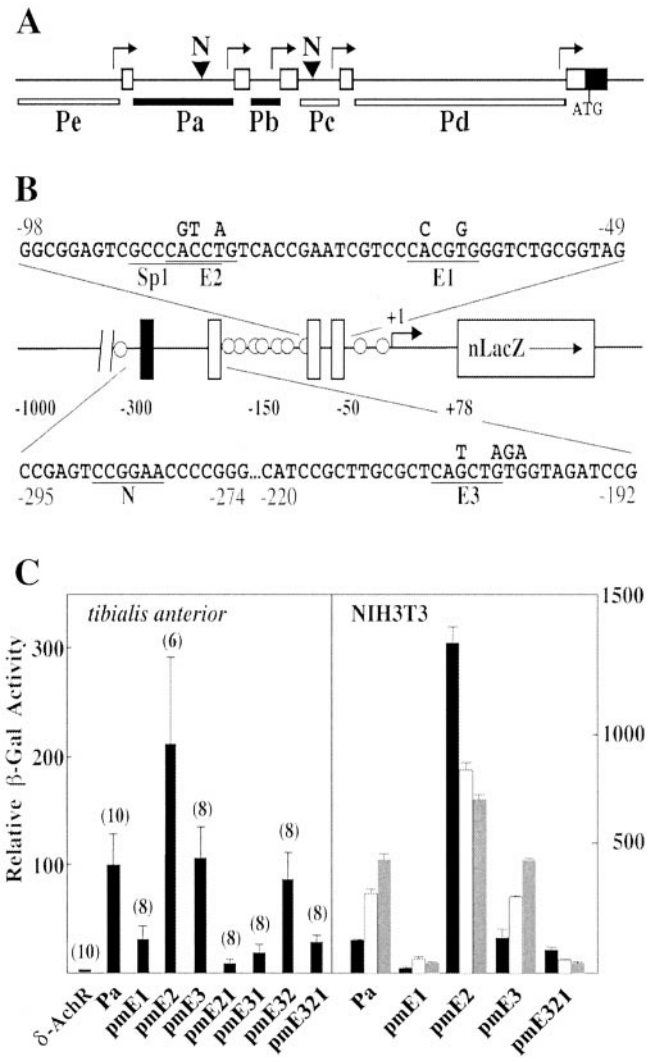

Fig. 1. E box-dependent basal activity and MyoD transactivation of the mouse RIα Pa promoter. (*A*) Structure of the 5′ region of the mouse RIα gene, containing five alternative promoters (Pa to Pe). Untranslated first exons are given as open boxes. The solid box represents coding sequences. Bent arrows indicate transcription start sites upstream of the first exons. Solid bars underline the region corresponding to the Pa and Pb promoters, which are active in adult skeletal muscle; the open bars indicate the other RIα promoters (Pc, Pd, and Pe). Arrowheads show the positions of N boxes. (*B*) Schematic representation of the Pa-nLacZ construct, containing the Pa promoter upstream of the β-gal reporter gene to which a nuclear localization signal has been added (nLacZ). The E and N boxes are represented as open and solid rectangles, respectively, and the consensus binding sites for ubiquitous transcription factors are indicated as circles. Sequences of the E and N boxes and the Sp1-binding site are underlined, and mutations introduced into the E boxes are given. (*C*) Effects of the mutations on basal and MyoD-enhanced expression of the β-gal reporter gene. (*Left*) Normalized β-gal activities of total extracts of injected, nonregenerating *tibialis anterior* muscles expressed as mean values relative to the activity of nonmutated Pa-nLacZ (set to 100). Numbers of injected muscles are indicated in parentheses. (*Right*) Normalized β-gal activities of NIH 3T3 fibroblast cells cotransfected with the β-gal reporter constructs and different amounts of a MyoD expression vector (solid, shaded, and open histograms correspond to 0, 0.5, and 2 μg, respectively). Activities relative to Pa-nLacZ (set to 100) are mean values (SD of two independent experiments with duplicate samples).

with small numbers of stained nuclei after overnight incubation, mostly at NMJ sites (data not shown). The rapid staining in a large number of fibers of muscles injected with the Pa-nLacZ plasmid leads us to speculate that any subsynaptic expression conferred by the N box element would be masked in the context of such a strong promoter.

Activity of the RIα Pa Promoter Involves E Boxes. The ability of the strong Pa promoter to respond to activation by myogenic transcription factors was examined in transient cotransfection assays with a MyoD expression vector in NIH 3T3 fibroblast and C2/7 myoblast cells. The Pb-nLacZ plasmid was used as a non-E box-containing control. Pa activity was enhanced by MyoD up to 6-fold (NIH 3T3, Fig. 1*C*) and 18-fold (C2/7) in a dose-dependent manner whereas Pb was not (data not shown). Moreover, whereas Pb is 6- to 7-fold more active than Pa in NIH 3T3 cells, this difference in promoter strength was reduced in cells cotransfected with MyoD, resulting in the 1a/1b ratio of 1.5 that we have reported previously for RIα transcripts in adult skeletal muscle (14). These results show that Pa contains regulatory elements necessary not only for ubiquitous expression but for muscle-enhanced expression as well.

Mutations of the E Boxes Alter Pa Activity. To determine the roles of the E boxes, we introduced mutations (Fig. 1*B*) that abolish protein binding. Pa-nLacZ and the E box mutant plasmids were injected into intact muscle and reporter gene activities were measured. Mutations of the E1 box (pE1m) decreased Pa activity by around 70% (Fig. 1*C*). In contrast, the pE2m plasmid conferred a 2-fold higher activity than Pa, suggesting that the E2 box acts as a repressor element. Mutations of the E3 box (pE3m) had no effect. Simultaneous mutations in E1 and E2 resulted in activity similar to that obtained by mutating E1 alone, indicating that E1 has a dominant effect over the dampening activity mediated by E2. The effects of these mutations also were examined in transiently transfected NIH 3T3 (Fig. 1*C*) or C2/7 cells (data not shown). The patterns of activity of the different β-gal reporter constructs were similar to those observed in whole muscle, suggesting that similar mechanisms regulate the Pa promoter in the two situations.

Cotransfections of the test plasmids with different amounts of MyoD expression vector into NIH 3T3 (Fig. 1*C*) or C2/7 cells (data not shown) revealed that mutations of the E1 box abolished transactivation whereas the E3 box mutation had no effect. Surprisingly, the increased basal expression observed for the E2 box-mutated plasmid was decreased by MyoD without falling below the MyoD-induced level obtained for the wild-type Pa plasmid. These results indicate that both basal and MyoD-induced activity of the Pa promoter require the E1 and E2 elements.

USF Proteins Bind to E1. The identification of the E1-binding proteins was performed by EMSA (Fig. 2*A*) by using a probe encompassing the −49- to −69-nt region of Pa. A major (band I) and a minor (band II) complex were detected with fibroblast and myotube nuclear extracts (lanes 1 and 2). Mutation of E1 abolished the formation of both complexes, and the intensity of the bands diminished in the presence of an excess of unlabeled probe but was not affected by a MyoD-binding site (mckR) or preincubation with anti-MyoD antibody (data not shown). In contrast, competition experiments with an oligonucleotide bearing a USF-binding site (MLP) decreased the intensity of complexes I and II for both extracts (lanes 3 and 4).

The USF family contains three members: USF2a and USF2b, which are generated by alternative splicing, and USF1 (18). These factors bind DNA as homo- or heterodimers but do not associate with the myogenic factors (29). Incubation of nuclear proteins from fibroblasts or myotubes with anti-USF2 or anti-USF1 antibodies revealed that complexes I and II contain the different USF proteins (lanes 5–9).

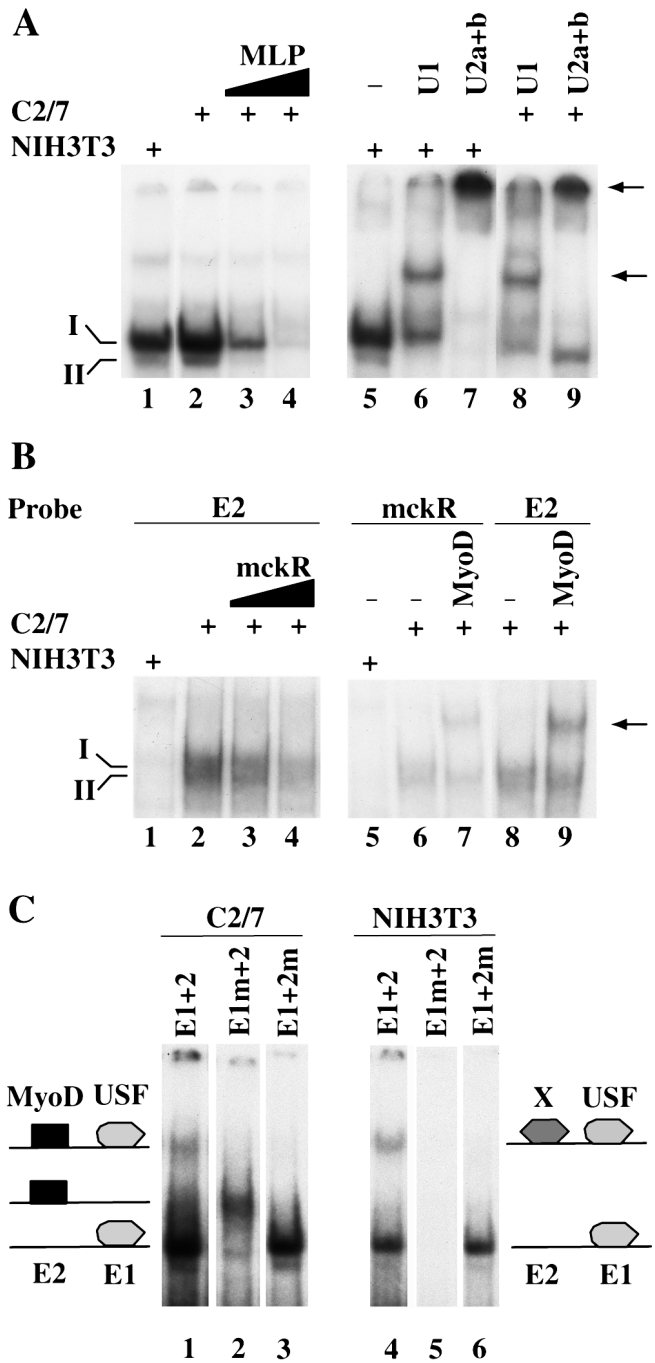

Fig. 2. Proteins binding to the E1 and E2 boxes of promoter Pa. NIH 3T3 fibroblast and C2/7 myotube nuclear extracts were incubated with radiolabeled, double-stranded oligonucleotides encompassing the E1 box (*A*), the E2 box or mckR (*B*), and E1 + E2 (*C*). Complexes were resolved in 4% acrylamide gels. Competitions were performed with a 10- and 50-fold molar excess of unlabeled oligonucleotide MLP (USF-binding site) or mckR (MyoD-binding site). Supershifted complexes resulting from preincubation with either MyoD, USF1 (U1), or USF2 (U2) antibodies are indicated by arrows.

Myogenic Factors Bind to E2. Proteins binding to E2 (Fig. 2*B*) were characterized by using a probe spanning −68 to −98 nt. With myotube extracts, two bands (lanes 2 and 8) were detected that were similar to those obtained with the control mckR probe (lane 6). Formation of both complexes was blocked by an excess of unlabeled E2 or mckR (lanes 3–4) whereas neither was detectable with NIH 3T3 extracts (lanes 1 and 5) or a mutated

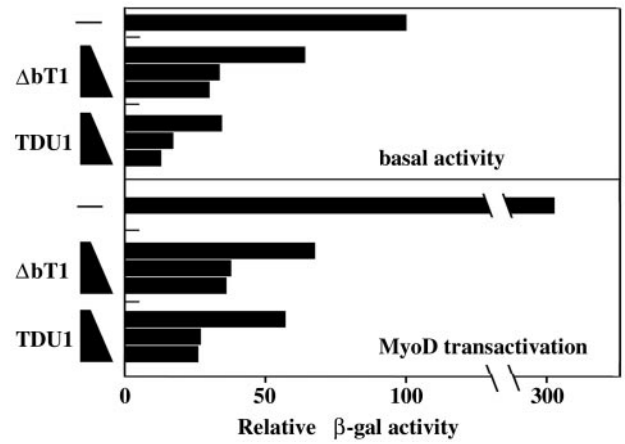

Fig. 3. Dependence on USF of Pa basal and MyoD-mediated activity. NIH 3T3 cells were cotransfected with Pa-nLacZ and different amounts (0.05, 0.5, and 2 μg) of expression vectors encoding truncated forms of USF1 either lacking the DNA-binding (DbT1) or the transactivation domain (TDU1). To each sample, 2 μg of the MyoD expression vector (*Lower*) or the vector lacking the MyoD-coding region (*Upper*) was added. β-Gal activities, expressed relative to activity in the absence of MyoD and truncated USF proteins (set at 100), are mean values of two experiments.

E2 probe (data not shown). Anti-MyoD antibody decreased the intensity of band I (lanes 7 and 9), but not of band II, showing that only complex I contains MyoD. Because myogenin is implicated in the formation of complex II with the mckR probe (34), complex II may be a result of myogenin binding to the E2 probe.

Protein Binding to E2 in the Absence of MyoD Requires USF Bound to E1. Simultaneous protein binding was monitored (Fig. 2*C*) with a probe containing both E1 and E2 (−49 to −98 nt). With C2/7 extracts, in addition to the two faster-migrating bands, which were blocked with USF- and MyoD-binding sites, a slower-migrating band was detected (lane 1). Competition and supershift assays showed that this complex is formed by binding of both USF and MyoD. Furthermore, the mutation of either E box revealed that binding of USF and MyoD occurred independently (lanes 2 and 3). In contrast, the binding of NIH 3T3 proteins generated only one faster and a slower migrating band (lane 4). Mutation of E1 abolished formation of both complexes (lane 5) whereas mutation in E2 prevented formation only of the slower-migrating band (lane 6). These results suggest that the slower-migrating complex is formed by protein binding to E2 in a USF/E1 complex-dependent manner. Mutations of E2 also affect an overlapping Sp1-binding site (Fig. 1*B*). We therefore investigated whether Sp1 could be bound to E2. However, preincubation with anti-Sp1 antibodies did not interfere with formation of the slower-migrating complex (data not shown). Because E boxes bind proteins containing a bHLH domain, the E2-binding protein likely belongs to this family. Inhibitory bHLH proteins that compete with MyoD for DNA binding have been described and include MyoR (35), Mist1 (36), the mouse snail-related gene, Smuc (37), and the E1A/E12 heterodimer (38).

MyoD Transactivation Requires USF/E1 Complex Activity. Contribution of the USF proteins to MyoD transactivation of Pa was assessed in transient cotransfections of NIH 3T3 cells with MyoD and truncated forms of USF either lacking the DNA-binding domain (DbT1) or the transactivation domain (TDU1) (22). Expression of dominant-negative forms of either USF1 (Fig. 3) or USF2 proteins (data not shown) decreased the basal expres-

sion of the β-gal reporter gene and abolished MyoD transactivation. Thus, basal activity and MyoD transactivation depend on both DNA binding and transactivation capacity of the USF proteins.

According to all these observations, we propose a model that could account for muscle-enhanced expression involving cooperation between myogenic and nonmyogenic factors. In the absence of MyoD, a protein bound to E2 could temper the transcriptional activation by USF. Mutation of E2, by abolishing binding of the putative repressor, would lead to increased transcriptional activity. MyoD transactivation appears to result from replacement of the repressor. In the presence of MyoD, activity decreases in the E2-mutated context, suggesting that MyoD also dampens USF activity. The inhibitory effects of MyoD on the activity of USF observed for the Pa promoter is in contrast with the positive cooperation between myogenic and USF proteins involved in the response to denervation of the chicken AChR α-subunit gene (29). Our model also could apply to other cases of tissue-enhanced expression from the Pa promoter (14), assuming the participation of other tissue-specific bHLH transcription factors.

The Dimerization Domain of RIα Directs Its Accumulation at the NMJ. We showed previously that the RIα protein is enriched at the NMJ (6). To study this targeting, we used *in vivo* injections into muscles of plasmids encoding RIα-GFP fusion proteins driven by a viral promoter (Fig. 4*A*). *In vivo* injection has been used to define transcriptional mechanisms that govern subsynaptic expression (19, 32, 33) but not to study protein localization. Expression of GFP alone (pEGFP-N3) resulted in diffuse fluorescence throughout the cytoplasm (Figs. 4*A* and 5). In contrast, the RIα-GFP fusion protein (pRIα-GFP) accumulated in green dots at and around the NMJ in 77% of the expressing fibers. Type I PKA can be recruited by activated epidermal growth factor receptor through interaction of a proline-rich region of RIα (residues 82–91) with the SH3 domains of the Grb2 adapter protein (39). However, this proline stretch is not required for the accumulation of the fusion proteins because deletion of this region in pRIα (1–81)-GFP did not abolish localization (Figs. 4*A* and 5). These results indicate that the first 81 residues of RIα, containing the dimerization domain, are sufficient for synaptic localization. This enrichment occurs irrespective of the site of reporter gene transcription because expression of all three fusion proteins controlled by the AChR δ-subunit promoter gave identical results (data not shown). The dimerization domain of RIα also is implicated in its localization in sensory cells in the ear and retina through interactions with the unconventional myosin VIIA (40).

The Dimerization/Docking Domain of RIIα Does Not Confer NMJ Localization. The dimerization domain of the RIα subunit has been defined as a docking domain for the *in vitro* interaction with D-AKAPs (8, 9, 41) via an α-helix, which shares similarities with the high-affinity AKAP-binding site of RII subunits (42). However, the first 44 aa of RIIα, which contain the structural determinants for dimerization and interaction with AKAPs, do not confer NMJ localization of the RIIα-GFP fusion protein (Figs. 4*A* and 5). RIIα(1–44)-GFP protein-expressing muscle fibers show perinuclear or nuclear enrichment of GFP fluorescence (Fig. 4*A*), implying its recruitment by an AKAP at this site as reported previously for cardiac myocytes (43).

NMJ Anchoring Requires RIα Residues Conserved Between Mammalian and Nematode Subunits. The dimerization domains of RIα and RII subunits show striking similarities in secondary structure because the N-terminal segment of both subunit types includes two α-helices (44). The structure and function of the distal dimerization helix (residues 49–64 in RIα) are highly conserved

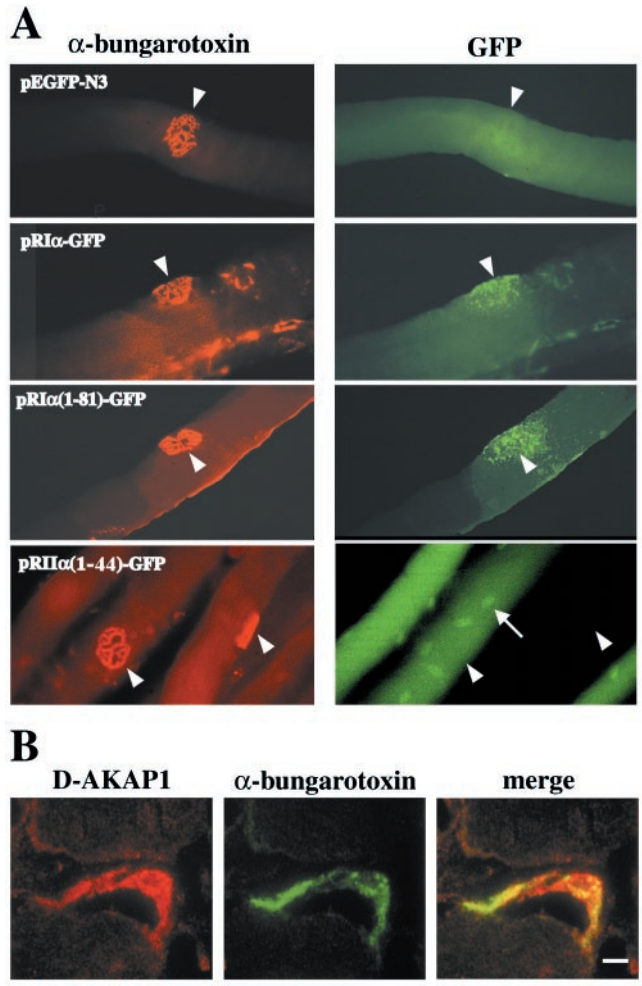

Fig. 4. Accumulation of RIα-GFP fusion proteins and of D-AKAP1 at the NMJ. (*A*) The dimerization domain of RIα, but not of RIIα, is able to direct NMJ localization. Plasmids encoding full-length or truncated RIα-GFP or RIIα(1–44)-GFP fusion proteins were injected into *tibialis anterior* muscles. Whole fibers expressing GFP were dissected and stained with tetramethylrhodamine B isothiocyanate-α-bungarotoxin to reveal the NMJ (open arrowheads). A fiber negative for GFP is shown in *Lower Right*. The arrow points to a nucleus in the multinucleated muscle fiber. (*B*) Confocal microscopy images of an adult muscle NMJ double-stained with anti-D-AKAP1 antibody and FITC-α-bungarotoxin. The photos show a single optical slice. (Bar = 5 μm.)

between RIα and RII. Substitution of Phe-54 with Ala in the full-length RIα-GFP fusion protein abolished anchoring to the NMJ (Fig. 5). Because aromatic amino acids at this position are indispensable for maintaining the overall dimeric structure of R subunits, this result indicates that dimerization of RIα is required for NMJ anchoring.

However, residues in the proximal helix (residues 18–44) required for docking function are not conserved between RI and RII. Indeed, side chains from hydrophobic amino acids in the docking region of RII engage in contacts with apolar core residues in the tethering domain of classical mammalian AKAPs (45). In *C. elegans*, the RI-like R_{CE} subunit contains a proximal helix that mediates high-affinity binding with the tethering domain of the isoform-selective anchor protein $AKAP_{CE}$. Side chains from Cys-23, Val-27, Ile-32, and Cys-44 assemble a hydrophobic surface that interacts with a complementary nonpolar-binding pocket in the $AKAP_{CE}$ (11). These amino acids are conserved in the mammalian RIα subunits. Mutation of the corresponding Val-22 to Ala in the mouse RIα protein led to a

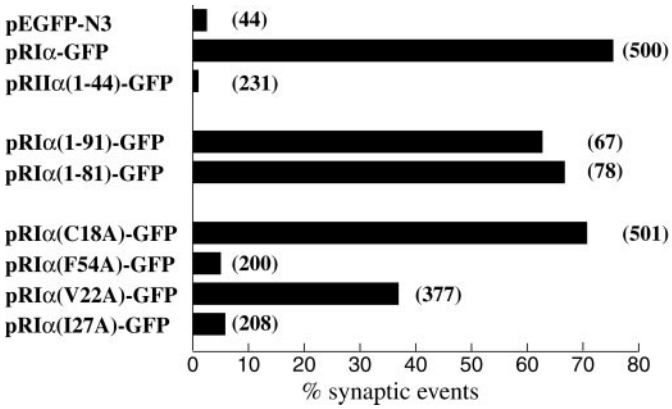

Fig. 5. Structural determinants of RIα required for its NMJ enrichment. Percentage of coincidence of tetramethylrhodamine B isothiocyanate-α-bungarotoxin and GFP fluorescence was obtained with plasmids encoding full-length RIα(pRIα-GFP), N-terminal sequences of RIα(residues 1–91 or 1–81) or of RIIα (residues 1–44), and single amino acid substitutions of full-length RIα (C18A, V22A, I27A, F54A). The number of GFP-positive fibers examined for each construct is indicated in parentheses.

50% decrease in frequency of synaptic accumulation whereas substitution of Ile-27 abolished localization at the NMJ; the mutation of Cys-18 to Ala had no effect (Fig. 5). Taken together, our data demonstrate that Val-22, Ile-27, and Phe-54 are necessary for recruitment of the mouse RIα subunit.

D-AKAP1 Is Enriched at the NMJ. The residues we have defined as critical for the NMJ localization of RIα, Val-22, Ile-27, and Phe-54, also are required for its interaction with D-AKAP1 *in vitro* (13). To determine whether D-AKAP1 could be implicated in maintaining RIα at the NMJ, its distribution on *tibialis anterior* muscle sections was analyzed by immunofluorescence by using an anti-D-AKAP1 antibody (Fig. 4*B*). Simultaneous labeling with FITC-coupled α-bungarotoxin and confocal microscopic analysis demonstrated an enrichment of D-AKAP1 at the NMJ and a partial colocalization of the two signals. Similar colocalization has been observed by G. Perkins and S. S. Taylor by using affinity-purified antibody (personal communication). In addition, two other polyclonal antibodies directed against different portions of D-AKAP1 gave the same results (data not shown). Consequently, D-AKAP1 could be responsible for targeting of RIα to the NMJ. Exclusion of RIIα from the NMJ was unexpected because D-AKAP1 exhibits higher affinity for RII than RI *in vitro* (9). However, the discrepancy could be due to the presence in the nuclear area of an AKAP that exhibits higher affinity for RIIα and, consequently, could preferentially recruit RIIα. Alternatively, other D-AKAPs or proteins homologous to $AKAP_{CE}$ could be involved in anchoring type I PKA regulatory subunits.

We thank numerous colleagues who have aided us: Marguerite Lemonnier, Laurent Schaëffer, and Susan S. Taylor for helpful discussions and for materials; Susan S. Taylor and Guy Perkins for permission to cite unpublished results; for materials, Arlette Cohen, Shahragim Tajbakhsh, Kjetil Taskén, and Benoît Viollet; and for confocal microscopy, Raymond Hellio. S.B. was supported by a fellowship from La Fondation pour la Recherche Médicale.

1. Colledge, M. & Scott, J. D. (1999) *Trends Cell Biol.* **9,** 216–221.
2. Dell'Acqua, M. L. & Scott, J. D. (1997) *J. Biol. Chem.* **272,** 12881–12884.
3. Rubin, C. S., Erlichman, J. & Rosen, O. M. (1972) *J. Biol. Chem.* **247,** 6135–6139.
4. Skålhegg, B. S., Taskén, K., Hansson, V., Huitfeldt, H. S., Jahnsen, T. & Lea, T. (1994) *Science* **263,** 84–87.
5. Miki, K. & Eddy, E. M. (1998) *J. Biol. Chem.* **273,** 34384–34390.
6. Imaizumi-Scherrer, T., Faust, D. M., Bénichou, J. C., Hellio, R. & Weiss, M. C. (1996) *J. Cell. Biol.* **134,** 1241–1254.
7. Imaizumi-Scherrer, T., Faust, D. M., Barradeau, S., Hellio, R. & Weiss, M. C. (2001) *Exp. Cell Res.*, in press.
8. Huang, L. J., Durick, K., Weiner, J. A., Chun, J. & Taylor, S. S. (1997) *Proc. Natl. Acad. Sci. USA* **94,** 11184–11189.
9. Huang, L. J., Durick, K., Weiner, J. A., Chun, J. & Taylor, S. S. (1997) *J. Biol. Chem.* **272,** 8057–8064.
10. Angelo, R. & Rubin, C. S. (1998) *J. Biol. Chem.* **273,** 14633–14643.
11. Angelo, R. G. & Rubin, C. S. (2000) *J. Biol. Chem.* **275,** 4351–4362.
12. Wolff, J. A., Malone, R. W., Williams, P., Chong, W., Acsadi, G., Jani, A. & Felgner, P. L. (1990) *Science* **247,** 1465–1468.
13. Banky, P., Huang, L. J. & Taylor, S. S. (1998) *J. Biol. Chem.* **273,** 35048–35055.
14. Barradeau, S., Imaizumi-Scherrer, T., Weiss, M. C. & Faust, D. M. (2000) *FEBS Lett.* **476,** 272–276.
15. Apone, S. & Hauschka, S. D. (1995) *J. Biol. Chem.* **270,** 21420–21427.
16. Edmondson, D. G. & Olson, E. N. (1993) *J. Biol. Chem.* **268,** 755–758.
17. Lassar, A. B., Buskin, J. N., Lockshon, D., Davis, R. L., Apone, S., Hauschka, S. D. & Baltimore, D. (1989) *Cell* **58,** 823–831.
18. Viollet, B., Lefrançois-Martinez, A. M., Henrion, A., Kahn, A., Raymondjean, M. & Martinez, A. (1996) *J. Biol. Chem.* **271,** 1405–1415.
19. Koike, S., Schaëffer, L. & Changeux, J.-P. (1995) *Proc. Natl. Acad. Sci. USA* **92,** 10624–10628.
20. Catala, F., Wanner, R., Barton, P., Cohen, A., Wright, W. & Buckingham, M. (1995) *Mol. Cell. Biol.* **15,** 4585–4596.
21. Kingston, R. E., Chen, C. A., Okayama, H. & Rose, J. K. (1996) in *Current Protocols in Molecular Biology,* ed. Chanda, V. B. (Wiley, New York), pp. 9.1.4–9.1.9.
22. Lefrançois-Martinez, A. M., Martinez, A., Antoine, B., Raymondjean, M. & Kahn, A. (1995) *J. Biol. Chem.* **270,** 2640–2643.
23. Dignam, J. D., Leibowitz, R. M. & Roeder, R. G. (1983) *Nucleic Acids Res.* **11,** 1475–1489.
24. Vaulont, S., Puzenat, N., Levrat, F., Cognet, M., Kahn, A. & Raymondjean, M. (1989) *J. Mol. Biol.* **209,** 205–219.
25. Kelly, R. G., Zammit, P. S., Schneider, A., Alonso, S., Biben, C. & Buckingham, M. (1997) *Dev. Biol.* **187,** 183–199.
26. Huang, L. J., Wang, L., Ma, Y., Durick, K., Perkins, G., Deerinck, T. J., Ellisman, M. H. & Taylor, S. S. (1999) *J. Cell Biol.* **145,** 951–959.
27. Piette, J., Bessereau, J. L., Huchet, M. & Changeux, J.-P. (1990) *Nature (London)* **345,** 353–355.
28. Duclert, A., Savatier, N., Schaëffer, L. & Changeux, J.-P. (1996) *J. Biol. Chem.* **271,** 17433–17438.
29. Bessereau, J. L., Laundenbach, V., Le Poupon, C. & Changeux, J.-P. (1998) *J. Biol. Chem.* **273,** 12786–12793.
30. Duclert, A. & Changeux, J.-P. (1995) *Physiol. Rev.* **75,** 339–368.
31. Sanes, J. R. & Lichtman, J. W. (1999) *Annu. Rev. Neurosci.* **22,** 389–442.
32. Duclert, A., Savatier, N. & Changeux, J.-P. (1993) *Proc. Natl. Acad. Sci. USA* **90,** 3043–3047.
33. Gramolini, A. O., Angus, L. M., Schaëffer, L., Burton, E. A., Tinsley, J. M., Davies, K. E., Changeux, J.-P. & Jasmin, B. J. (1999) *Proc. Natl. Acad. Sci. USA* **96,** 3223–3227.
34. Lin, H. & Konieczny, S. F. (1992) *J. Biol. Chem.* **267,** 4773–4780.
35. Lu, J., Webb, R., Richardson, J. A. & Olson, E. N. (1999) *Proc. Natl. Acad. Sci. USA* **96,** 552–557.
36. Lemercier, C., To, R. Q., Carrasco, R. A. & Konieczny, S. F. (1998) *EMBO J.* **17,** 1412–1422.
37. Kataoka, H., Murayama, T., Yokode, M., Mori, S., Sano, H., Ozaki, H., Yokota, Y., Nishikawa, S. & Kita, T. (2000) *Nucleic Acids Res.* **28,** 626–633.
38. Taylor, D. A., Kraus, V. B., Schwarz, J. J., Olson, E. N. & Kraus, W. E. (1993) *Mol. Cell. Biol.* **13,** 4714–4727.
39. Tortora, G., Damiano, V., Bianco, C., Baldassarre, G., Bianco, A. R., Lanfrancone, L., Pelicci, P. G. & Ciardiello, F. (1997) *Oncogene* **14,** 923–928.
40. Küssel-Andermann, P., El-Amraoui, A., Safieddine, S., Hardelin, J.-P., Nouaille, S., Camonis, J. & Petit, C. (2000) *J. Biol. Chem.* **275,** 29654–29659.
41. Leon, D. A., Herberg, F. W., Banky, P. & Taylor, S. S. (1997) *J. Biol. Chem.* **272,** 28431–28437.
42. Carr, D. W., Stofko-Hahn, R. E., Fraser, I. D., Bishop, S. M., Acott, T. S., Brennan, R. G. & Scott, J. D. (1991) *J. Biol. Chem.* **266,** 14188–14192.
43. Kapiloff, M. S., Schillace, R. V., Westphal, A. M. & Scott, J. D. (1999) *J. Cell. Sci.* **112,** 2725–2736.
44. Banky, P., Newlon, M. G., Roy, M., Garrod, S., Taylor, S. S. & Jennings, P. A. (2000) *J. Biol. Chem.* **275,** 35146–35152.
45. Hausken, Z. E., Coghlan, V. M., Hastings, C. A., Reimann, E. M. & Scott, J. D. (1994) *J. Biol. Chem.* **269,** 24245–24251.